Phycologia

ISSN: 0031-8884 (Print) 2330-2968 (Online) Journal homepage: https://www.tandfonline.com/loi/uphy20

Surviving the marine environment: two new species of *Mallomonas* (Synurophyceae)

Minseok Jeong, Jong Im Kim, Bok Yeon Jo, Han Soon Kim, Peter A. Siver & Woongghi Shin

To cite this article: Minseok Jeong, Jong Im Kim, Bok Yeon Jo, Han Soon Kim, Peter A. Siver & Woongghi Shin (2019): Surviving the marine environment: two new species of *Mallomonas* (Synurophyceae), Phycologia, DOI: 10.1080/00318884.2019.1565718

To link to this article: https://doi.org/10.1080/00318884.2019.1565718

PHYCOLOGIA
https://doi.org/10.1080/00318884.2019.1565718

Surviving the marine environment: two new species of *Mallomonas* (Synurophyceae)

Minseok Jeong[1], Jong Im Kim[1], Bok Yeon Jo[2], Han Soon Kim[3], Peter A. Siver[4], and Woongghi Shin[1]

[1]*Department of Biology, Chungnam National University, Daejeon 34134, Korea*
[2]*Nakdonggang National Institute of Biological Resources, Sangju 37242, Korea*
[3]*School of Life Science, Kyungpook National University, Daegu 41566, Korea*
[4]*Department of Botany, Connecticut College, 270 Mohegan Ave., Box 5604, New London, Connecticut 06320, USA*

ABSTRACT

The genus *Mallomonas* consists of single-celled flagellates covered with siliceous scales and bristles and is well known in freshwater environments. Two new marine *Mallomonas* species were collected from Dongho Beach, Jeollabukdo, Korea. To fully understand the taxonomy of the new species, we performed molecular phylogenetic analysis based on a concatenated dataset and observed morphological features using light and electron microscopy. For the phylogenetic analysis, we used a combined dataset from five gene sequences: nuclear small subunit (SSU) and large subunit (LSU) rDNA and plastid LSU rDNA, *rbc*L and *psa*A genes. The new species *M. cuspis sp. nov*. grouped with *M. heterospina* and *M. oviformis* in the section *Planae*. It had scales with a broad shield marked with V-shaped internal ridge that lacked submarginal ribs and a dome. The other new species, *M. marina sp. nov*., clustered with *M. cratis, M. pseudocratis, M. asmundiae* and *M. striata* var. *serrata* in section *Striatae* and had scale characters that matched the group, including a well-developed posterior submarginal rib and series of transverse ribs on the shield and dome. In addition, we investigated the effect of salinity on growth rate and cell morphology. The two marine species represented high growth rate between salinities of 10 and 30 psu, suggesting that both species are well adapted in marine environments. When exposed to salinities of 0 and 5 psu, they underwent cell enlargement.

ARTICLE HISTORY
Received 19 September 2018
Accepted 3 January 2019
Published online 4 April 2019

KEYWORDS
Growth rate; *Mallomonas*; Marine; New species; Phylogeny; Salinity; Synurophyte; Ultrastructure

INTRODUCTION

Mallomonas is the most speciose genus in the class Synurophyceae with about 200 taxa in 19 sections (Kristiansen 2002; Kristiansen & Preisig 2007; Siver 1991; Siver *et al.* 2015). The single-celled organism has two unequal flagella and on most species only one is emergent from the cell. The cell is covered with siliceous scales and bristles that are intricate and highly organised (Kristiansen 2002; Siver 1991; Siver & Glew 1990). The scales are flat to slightly convex plate-like structures with a variety of designs that form the basis for inter- and infraspecies differentiation (Kristiansen 2005; Siver 1991, 2018; Siver *et al.* 2013). In *Mallomonas*, ultrastructural characters of scales (presence or absence of V-rib and dome, secondary ornamentation) and bristles (type and position) are used to distinguish between taxa at section, series, species and variety ranks.

In an early parsimony analysis based on nuclear small subunit (SSU) rDNA and scale characteristics, the genus *Mallomonas* formed a monophyletic lineage with the synurophycean assemblage *Synura* and *Neotessella* (Lavau *et al.* 1997). A second phylogenetic analysis using a combined nuclear SSU rDNA and plastid *rbc*L sequence dataset supported monophyly of *Mallomonas* but not based solely on the *rbc*L gene (Andersen 2007). More recently, *Mallomonas* was recovered as a monophyletic assemblage among synurophycean genera using a combination of nuclear SSU and large subunit (LSU) rDNA and plastid *rbc*L genes (Jo *et al.* 2013). In addition, the phylogenetic analysis of *Mallomonas*, based on morphological features and molecular data, indicated that it was divided into two major clades according to the presence/absence of a V-rib on the siliceous scales and the type of bristle produced (Jo *et al.* 2011, 2013; Siver *et al.* 2015).

The vast majority of *Mallomonas* species are known from freshwater environments worldwide, where they often form important components of planktic communities (Siver 1993; Siver & Hamer 1989). Several species included in two culture strains of *M. papillosa* and *M. cratis* (see description of two CCMP476 and CCMP3275 strains on the National Center for Marine Algae and Microbiota website) were previously reported from freshwater to brackish environments, especially around the Baltic Sea (Ikävalko 1994; Ikävalko & Thomsen 1996; Němcová *et al.* 2016). Sampling sites in the Baltic Sea were either lakes near the shorelines or brackish waterbodies with salinities of below 5 psu due to freshwater inflow from both melting snow and ice and rivers. During multiple samplings of marine sand flats at low tide on the west coast of Korea in the winter to spring of 2013–2017, we established cultures of two *Mallomonas* species with different sized cells and covered with scales and bristles. Taxonomic studies of newly discovered *Mallomonas* species from marine environments will provide insight into species diversity and speciation of the photosynthetic species belonging to the

CONTACT Woongghi Shin shinw@cnu.ac.kr

Colour versions of one or more of the figures in the article can be found online at www.tandfonline.com/uphy.
Supplemental data for this article can be accessed on the publisher's website.

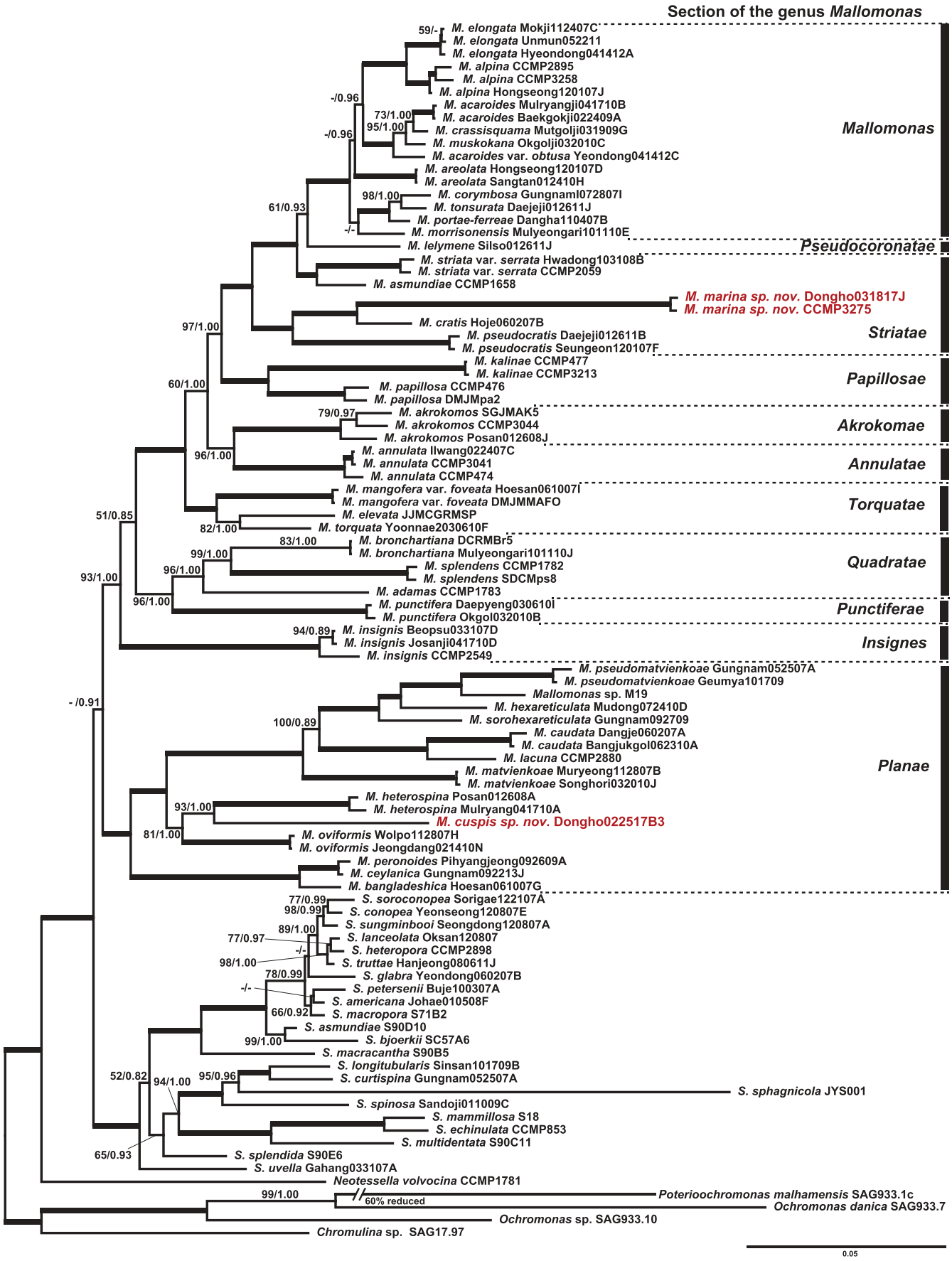

Fig. 1. Bayesian tree of *Mallomonas* based on combined nuclear SSU and LSU rDNA and plastid LSU rDNA, *rbc*L and *psa*A sequence data. The MLBS (left) and Bayesian PP (right) are shown on each node. Scale bar indicates number of substitutions per site; thick line indicates full support (100% bootstrap value for MLBS and 1.00 for PP) and (–) denotes values < 50% for MLBS or 0.70 for PP.

genus *Mallomonas*. Here, we describe two marine species, *M. cuspis sp. nov.* and *M. marina sp. nov.*, using light and electron microscopy coupled with molecular data.

MATERIAL AND METHODS

Culture

The marine *Mallomonas* species (*M. cuspis sp. nov.* Dongho022517B3, *M. marina sp. nov.* Dongho031817J) were collected at Dongho Beach, Jeollabukdo, Korea (35°31.00′N, 126°28.97′E, salinity value of 28.3 psu). We performed single cell isolation using a Pasteur capillary pipette and established them as unialgal culture strains. A second strain of *M. marina* CCMP3275 was obtained from the National Center for Marine Algae and Microbiota. All cultures were grown in DY-V medium (Andersen *et al.* 2005) with either distilled seawater or freshwater and were maintained at 17 °C using a 14:10-h light:dark cycle and light intensity of *c.* 30 µmol photon·m^{-2}·s^{-1} using cool-white fluorescent tubes (OSRAM Korea Co., Ansan, Korea). The information for each strain is listed in Table S1.

DNA extraction, amplification, sequencing and alignment

The cell was harvested by centrifugation (model 5424, Eppendorf, Hamburg, Germany) at 9391 × *g* for 3 min. Genomic DNA was extracted using a DOKDO-Prep Blood Genomic DNA Purification Kit (ELPIS-Biotech Inc., Daejeon, Korea). Polymerase chain reaction (PCR) was performed for five genes; nuclear SSU and LSU rRNA, plastid LSU rRNA, *rbc*L, and *psa*A. Specific primers were described by Jo *et al.* (2011, 2013) and *rbc*L primers were newly designed in this study: M46F-GAATCTGGAGTAATTCCATACAAA and M1397R-GATTTCCATAAATCTAAWGCWTCTTG. PCR was performed on a total volume of 25 µl; 1 µl of AccuPower PCR premix (Bioneer Co., Daejeon, Korea), 1 µl of forward primer, 1 µl of reverse primer, 2–5 µl of template DNA, and 17–20 µl of distilled water. The genes were amplified using a T100 Thermal Cycler (Bio-Rad Laboratories, Hercules, California USA). The first denaturation was run at 94 °C for 5 min, with 35 cycles of second denaturation at 94 °C for 30 s, annealing at 42–52 °C for 30 s to 1 min, extension at 72 °C for 1–2 min, and final extension at 72 °C for 7 min, and then held at 12 °C. All PCR products were purified using a Labopass PCR purification kit or Labopass gel purification kit (Cosmogenetech Co., Seoul, Korea) following the protocol given by the manufacturer. The purified PCR products were sequenced using an ABI PRISM (3730xL, Perkin-Elmer Applied Biosystems, Foster City, California USA). Alignment of sequences was performed visually using the Genetic Data Environment programme (Smith *et al.* 1994) based on the secondary structure of nuclear SSU rRNA of *M. annulata* and nuclear LSU rDNA of *Ochromonas danica* (Wuyts *et al.* 2001). The conserved regions of ribosomal DNA sequences were used for phylogenetic analysis and variation sites were excluded. For the *rbc*L gene, the first and second codons were used in phylogenetic analysis; the third codon was excluded due to multiple hits (Jo *et al.* 2011, 2013).

Phylogenetic analyses

A combined dataset of 9177 characters (nr SSU = 1,637, nr LSU = 2,547, pt LSU = 2,591, *rbc*L = 824 and *psa*A = 1,578) from 95 taxa was generated for phylogenetic analysis (Table S1). Primers and ambiguously aligned regions were not used in phylogenetic analyses. The sequences of four chrysophycean species were used as outgroup taxa to root the tree because these taxa have been proved to be basal and have formed a sister clade with the genera *Mallomonas, Synura* and *Neotessella* in previous studies (Jo *et al.* 2013, 2016; Siver *et al.* 2015). Maximum-likelihood (ML) phylogenetic analysis was performed using RAxML v8.2.4 (Stamatakis 2014), with the general time-reversible plus gamma (GTR + GAMMA) model. We used 1000 independent tree inferences, using the -# option of the programme to identify the best tree. Gamma correction values and the proportion of invariable sites of the combined dataset were obtained automatically by the programme. Maximum-likelihood bootstrap values (MLBS) were calculated using 1000 replicates with the same substitution model. Bayesian analyses were performed using MrBayes v3.2 (Ronquist *et al.* 2012); the best-fit model for the combined dataset was determined by the Bayesian information criterion of MODELTEST v3.7 (Posada & Crandall 1998), with general time-reversible plus gamma (GTR + I + G). Each analysis was performed using a Metropolis-coupled MarKov chain Monte Carlo approach, with 2,000,000 cycles for each chain. Trees were saved to a file every 1000 cycles, and the burn-in point was identified graphically by tracking the likelihoods (Tracer v1.5; http://tree.bio.ed.ac.uk/software/tracer/). A majority-rule consensus tree was created from the remaining 1500 trees to examine the posterior probabilities (PP) of each clade.

Light microscopy

Culture strains were observed and identified using an Axio Imager A2 microscope (Carl Zeiss Inc., Hallbergmoos, Germany) equipped with differential interference contrast optics. Images were captured with an AxioCam HRc (Carl Zeiss Inc.) photomicrographic system attached to the microscope. Cellular dimensions were determined by measuring 25–30 cells of each taxon from photographic images (Tables 1, 2).

Transmission electron microscopy

For scale ultrastructure of each strain, we collected approximately 100 cells per strain and put them into 1.5-ml microcentrifuge tubes. Cells were sonicated to detach scales and washed three times with distilled water. After centrifugation at 6010 × *g* for 1 min, the supernatant was discarded and 50 µl of distilled water (including the samples) remained. The remaining portions were mounted onto Formvar-coated copper grids and air dried. The grids were viewed in a JEM 1010 transmission electron microscope (TEM; JEOL Ltd., Tokyo, Japan) at 80 kV. Kodak EM Film 4489 (Eastman Kodak Co., Rochester, New York USA) was used to record scale morphology (Table 1).

Table 1. Summary of major characteristics of *Mallomonas* section *Planae* observed with electron microscope (EM).

Taxon	Cell size (μm)		Scales							
	Length	Width	Dome	V-ribs	Anterior submarginal ribs	Anterior flange	Posterior flange	Secondary structure on the shield	Specialised posterior pores	Bristle
M. bangladeshica[a]	15.75–18.98	9.39–11.48	–	–	–	–	–	+, Papillae, internal struts	–	Smooth shaft, needle-shaped apex
M. caudata[a]	37.05–66.67	19.38–28.00	–	–	–	–	–	–	+, One large pore in cluster of small pores	Distal part serration
M. ceylanica[b]	17–25	9–13	–	–	–	–	–	+, Papillae	–	Smooth shaft, needle-shaped apex
M. cuspis[c]	9.5–14.1	8.1–11.9	–	–	–	–	–	+, Internal struts	–	Smooth shaft, needle-shaped apex
M. heterospina[a]	15.56–16.25	10.25–12.50	+	–	–	–	–	+, Reticulum	–	Smooth shaft, needle-shaped or hooked apex
M. hexareticulata[a]	12.20–18.48	7.48–11.52	–	–	–	–	–	+, Hexagonal meshwork of secondary layer	+, One large pore in cluster of small pores	Divided into apex with several parts
M. lacuna[a]	36.07–67.37	15.68–20.02	–	–	–	–	–	–	+, One large pit	Distal part serration
M. matvienkoae[a]	14.25–18.41	8.25–16.22	–	–	–	–	–	+, Meshwork of secondary layer	+, One large pore in cluster of small pores	Expanded apex
M. oviformis[a]	18.55–22.00	16.60–21.25	–	–	–	–	–	+, Papillae	–	Smooth, trifurcate apex
M. peronoides[a]	12.34–24.83	8.22–12.56	–	–	–	–	–	+, Papillae, internal struts	–	Smooth shaft, needle-shaped apex
M. pseudomatvienkoae[a]	18.03–22.24	8.41–13.24	–	–	–	–	–	+, Meshwork of secondary layer	+, One large pore	Bifurcate apex
M. sorohexareticulata[a]	28.25–35.58	7.22–15.43	–	–	–	–	–	+, Papillae	+, One large pore	Expanded apex

[a]Jo *et al*. (2013).
[b]Dürrschmidt & Cronberg (1989).
[c]This study.

Table 2. Summary of major characteristics of *Mallomonas* section *Striatae* observed with electron microscope (EM).

Taxon	Cell size (μm)		Scales						Bristle
	Length	Width	Dome	V-ribs	Anterior submarginal ribs	Anterior flange	Posterior flange	Secondary structure on the shield	Specialised posterior pores	
M. cratis[a,b]	17–33	13–15	+	+, Teeth at the edge of V-rib hood	+	+, 3–7 struts	+, 16–23 struts	+, 14–18 transverse ribs	+, Group of small pores	Distal part serration
M. marina[c]	13.1–40.1	10.4–17.4	+	+	+	+, 4–8 struts	+, 18–26 struts	+, 13–20 regular transverse ribs	+, Group of three to five pores	Distal part serration
M. pseudocratis[a]	20–50	11–12	+	+	+	+, 5–6 struts	+, Incomplete struts	+, 10–15 transverse ribs	+, Group of small pores	Distal part serration
M. striata var. *serrata*[a]	12–28	9–10	+	+	+	+, 3–6 struts	+, 10–12 struts	+, 7–12 transverse ribs	+, Group of small pores	Distal part serration

[a]Jo *et al.* (2011).
[b]Siver (1991).
[c]This study.

Scanning electron microscopy

Cells were collected on 0.45-μm nylon membrane filters (Whatman Ltd., Maidstone, UK) and rinsed three times with DY-V seawater medium. Cells were fixed in 2.5% glutaraldehyde for 1 h and rinsed three times with DY-V seawater medium. Cells were then fixed in 1% OsO_4 for 1 h, dehydrated in ethanol series (50%, 60%, 70%, 80%, 90%, 100%) for 10 min at each step and dried in an HCP-2 critical-point dryer (Hitachi Co., Tokyo, Japan). Filters were mounted onto aluminium stubs with double-sided tape. Stubs were coated with platinum in a Cressington 208 High Resolution sputter coater (Dynavac, Polaron, UK) and viewed in a JSM 7000F field emission scanning electron microscope (SEM; JEOL Ltd.) at 5–10 kV.

Determining growth rate

The precultured salt concentration was 30 psu and two species were directly transferred to 30 ml of DY-V medium with different salt concentrations (0, 5, 10, 15, 20, 25, 30 psu). Two species were pre-adapted at each salt concentration for 7 days. Then 1 ml of culture aliquots from each salinity was transferred to three new replicate media with the same salinity. The salt concentration was determined by a YSI Pro 30 Conductivity metre (YSI Inc., Yellow Springs, Ohio USA). The cultures were grown at the same temperature and irradiance noted above. The 300-μl samples for cell counting were extracted twice from each culture in the morning every day for 10 days and enumerated with a haemocytometer. Growth rates were determined based on cell counts and calculated using the equation:

$$\text{Growth rate}(\mu) = \frac{\ln(count_2) - \ln(count_1)}{time_2 - time_1},$$

where $count_2$ is cell number at $time_2$ (final day) and $count_1$ is cell number at $time_1$ (initial day).

RESULTS

Phylogenetic analysis

ML and Bayesian analyses were conducted using the combine dataset of five genes from 95 taxa (Fig. 1, Table S1). *Mallomonas* was monophyletic and divided into two major clades according to the presence or absence of a V-rib (MLBS = 48, pp = 0.91). The section *Planae* without a V-rib included 12 species and one of the new species, *M. cuspis* (MLBS = 100, pp = 1.00). The new marine species *M. cuspis* was a sister taxon to *M. heterospina* (MLBS = 93, PP = 1.00). The other major clade bearing a V-rib was grouped with 10 sections: *Akrokomae, Annulatae, Insignes, Mallomonas, Papillosae, Psuedocoronatae, Punctiferae, Quadratae, Striatae*, and *Torquatae* (MLBS = 93, PP = 1.00). The second new marine species *M. marina* was grouped with *M. pseudocratis* and *M. cratis* in section *Striatae* (MLBS = 100, PP = 1.00) and was a sister taxon to *M. cratis* (MLBS = 100, PP = 1.00).

Morphology

Ultrastructural features of the scale and bristle for the two new *Mallomonas* species are summarised in Tables 1 and 2. *Mallomonas cuspis* had two golden plastids and one emergent

flagellum (Figs 2–4). It had elliptical or obovoid shaped scales, which were characterised by a V-shaped ridge at the centre of the shield, lack of a true V-rib, and smooth, needle-shaped bristles (Figs 8–13). *M. marina* had two golden plastids and one emergent, visible flagellum (Figs 5–7). It had elliptical scales, characterised by a V-rib, a dome with secondary structures, a series of evenly spaced transverse ribs, large pores on the shield, a posterior flange, and serrated bristles (Figs 14–21).

Mallomonas cuspis M.Jeong, J.I.Kim, B.Y.Jo, H.S.Kim, P.A. Siver & W.Shin *sp. nov.*

Figs 2–4, 8–13

DESCRIPTION: Cells were spherical to ovoid or obovoid, ranged in size from 9.5–14.1 × 8.1–11.9 µm, and were covered with oval scales. Two golden plastids were longitudinal along peripheral sides of the cell. A single emergent flagellum was visible (12.4 – 25.6 µm). The oval scales ranged from 2.5– 3.4 × 1.3–2.1 µm, without a submarginal rib structure and dome. A posterior rim encircled one third to half of the perimeter. Widely and randomly spaced small pores with variable shapes and diameters covered the base plate except for the anterior region. The middle region of the base plate was marked with a shallow, V-shaped internal ridge. Bristles covered the whole cell surface; bristles ranged from 3.2 to 7.6 µm long and were smooth, slightly curved, and tapered. The bristle shaft had a longitudinal slit and a pointed apex.

HOLOTYPE: Collection of specimens on SEM stub deposited at the Nakdonggang National Institute of Biological Resources, Sangju, Korea (NNIBR), NNIBROR1.

TYPE LOCALITY: Dongho Beach, Dongho-ri, Haeri-myeon, Kochang-gun, Jellabukdo, Korea (35°31.00′N, 126°28.97′E), 25 February 2017.

STRAIN TYPE: Dongho022517B3 deposited at NNIBR, FBCC200020D.

ETYMOLOGY: The Latin specific epithet '*cuspis*' refers to the arrowhead shaped (V-shaped) internal ridge of the scale.

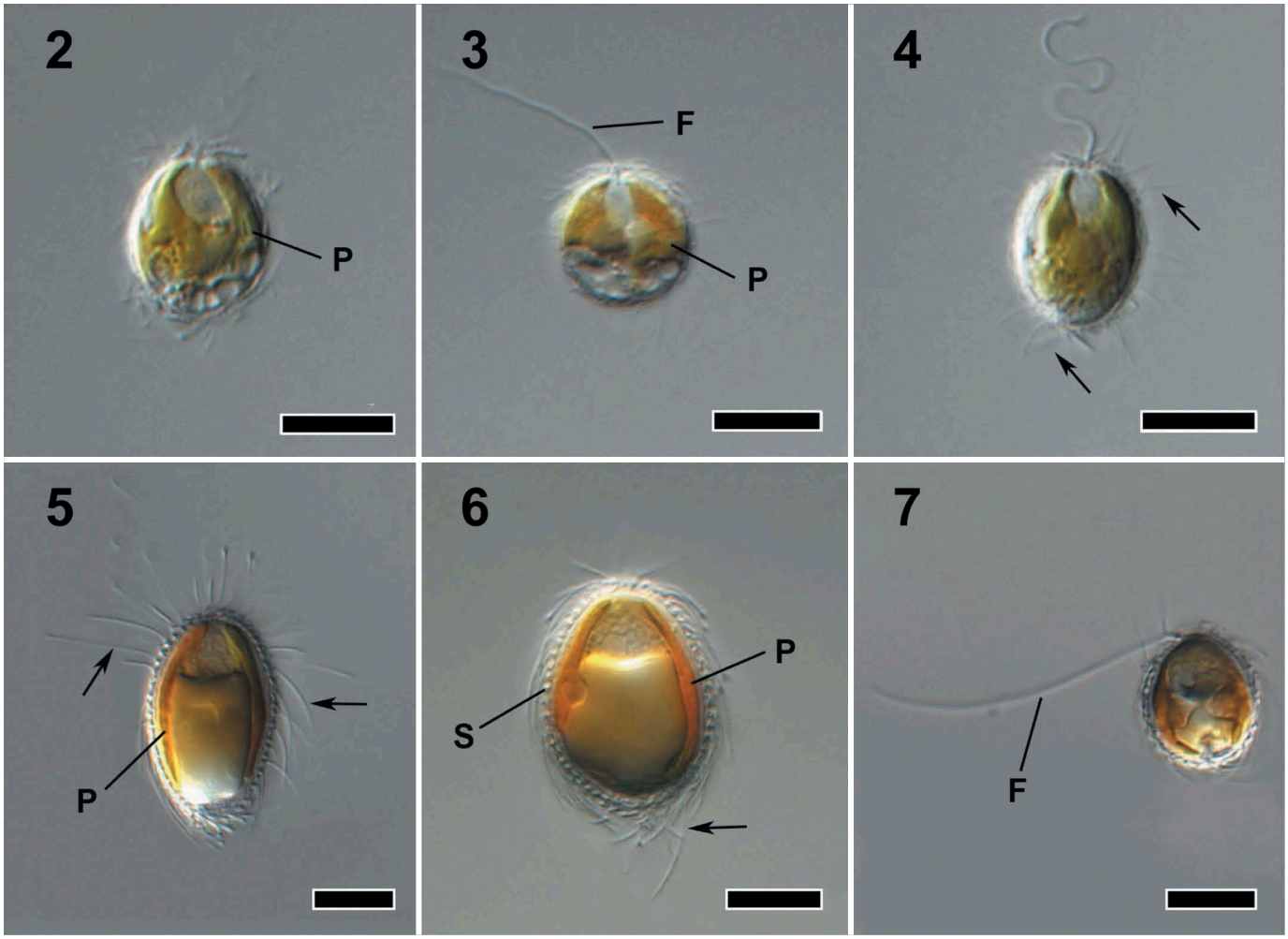

Figs 2–4. Light micrographs of *Mallomonas cuspis* Dongho022517B3. Scale bar = 10 µm.
Fig. 2. Ovoid cell with plastid (P) on both edges of cell.
Fig. 3. Spherical cell with plastid (P) and a long flagellum (F) stretching in front of cell.
Fig. 4. Obovoid cell with plastid, a long flagellum and bristle (arrows) stretching in all directions.
Figs 5–7. *M. marina* Dongho031817J. Scale bar = 10 µm.
Fig. 5. Elongated ovoid cell with plastid (P), scale and bristle (arrows) stretching in all directions. The appearance of cell covering structures is evident in LM.
Fig. 6. Ovoid cell with plastid, scale (S) and bristle (arrow) lying with their tip towards the posterior of the cell.
Fig. 7. Ovoid cell with a long flagellum (F).

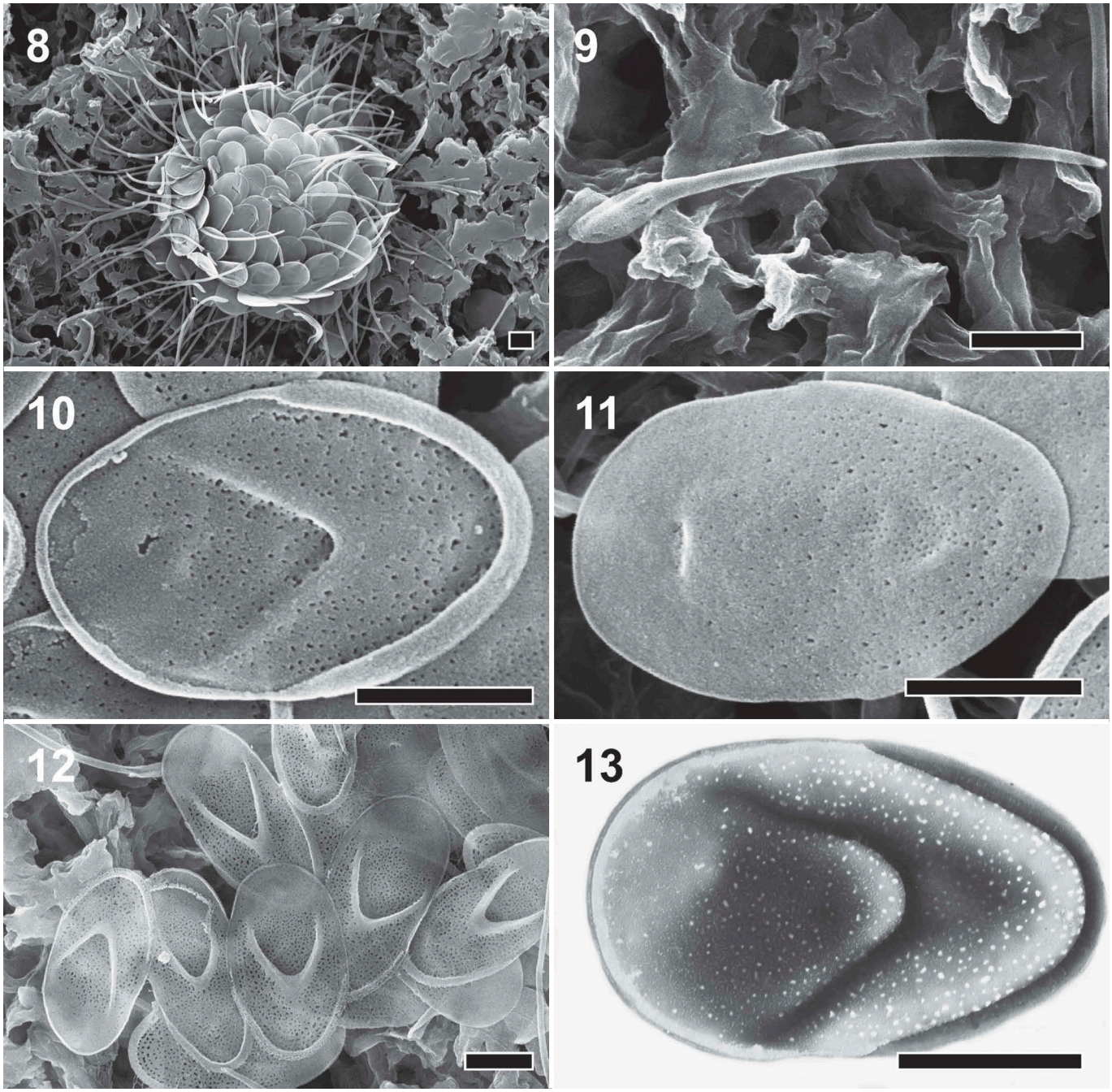

Figs 8–13. Cell, scale and bristle morphologies of *Mallomonas cuspis* Dongho022517B3. Scale bar = 1 μm.
Fig. 8. SEM image of spherical-shaped cell covered by scale and bristle.
Fig. 9. SEM image of smooth, needle-shaped bristle.
Fig. 10. SEM image of top surface of oval scale with V-shaped internal ridge, posterior rim and irregularly arranged small pores.
Fig. 11. SEM image of bottom surface of body scale with many small pores except for anterior region.
Fig. 12. SEM image of top surface of body scales.
Fig. 13. TEM image of body scale.

Mallomonas marina M.Jeong, J.I.Kim, B.Y.Jo, H.S.Kim, P. A.Siver & W.Shin *sp. nov.*

Figs 5–7, 14–21

DESCRIPTION: Cells were ovoid or obovoid to cylindrical, ranging in size from 13.14–40.1 × 10.4–17.4 μm, and were covered with elliptical tripartite scales and bristles. The two golden plastids were located in a peripheral position along peripheral sides of the cell. A single emergent flagellum was visible (30.6–58.1 μm). Scales ranged in size from 2.7–3.9 × 1.1–1.9 μm. The dome was marked with ribs arranged in irregular longitudinal or U-shaped patterns. The posterior rim of the scale encircled half to two-thirds of the scale perimeter and the shield was marked with 13–20 regularly spaced transverse ribs. The posterior region of the shield at the base of the V-rib was marked with three to five large pores. The V-rib was well developed and strongly hooded. The posterior flange was small and marked with a row of large pores close to the posterior rim. The anterior flange was winged with about four to eight struts. The arms of the V-rib extended to the anterior

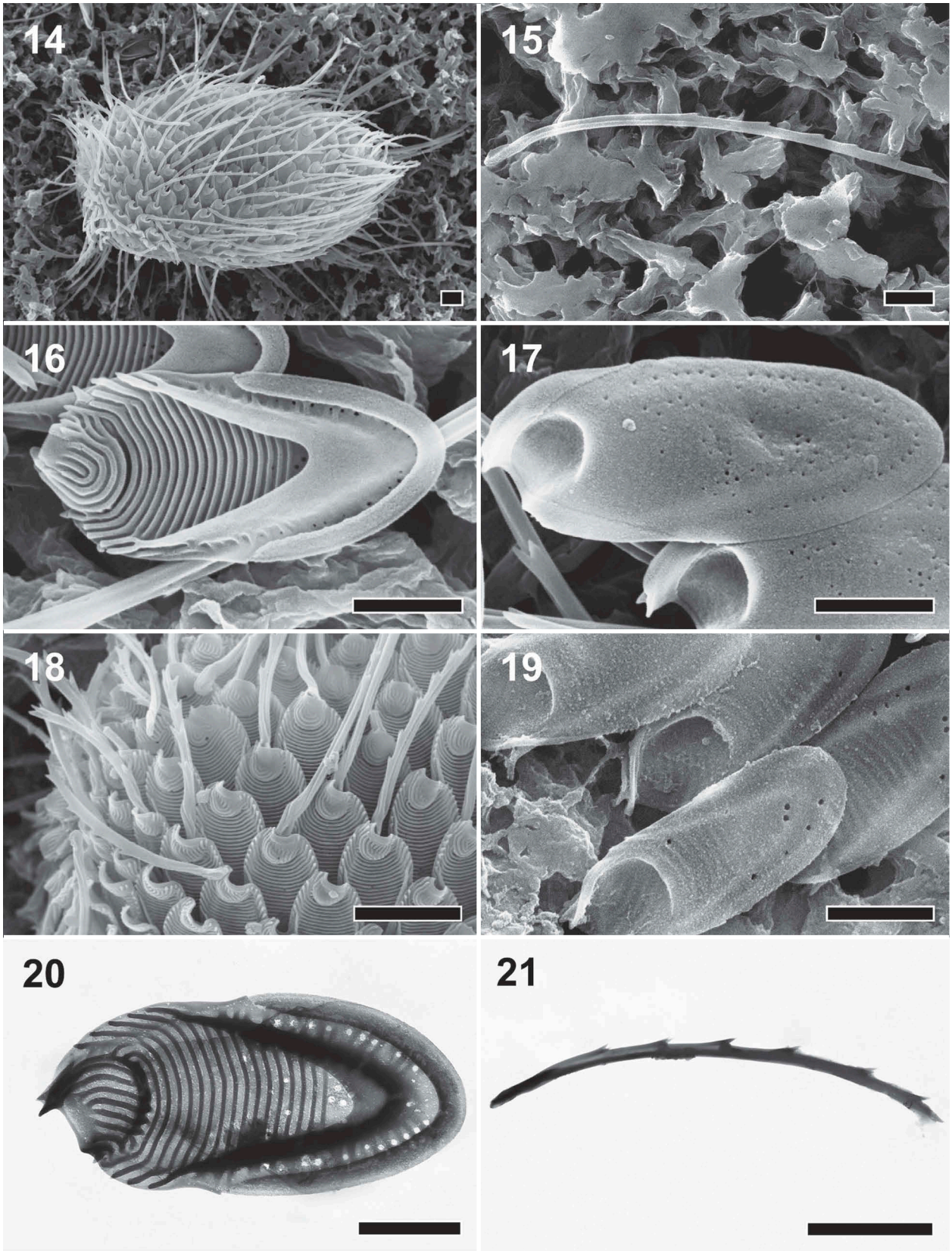

Figs 14–21. Cell, scale and bristle morphologies of *Mallomonas marina* Dongho031817J). Scale bar = 1 µm.
Fig. 14. SEM image of obovoid cell covered by scale and bristle.
Fig. 15. SEM image of serrated bristle.
Fig. 16. SEM image of top surface of body scale having posterior submarginal rib, pores along the posterior rib, struts, transverse rib, and dome with secondary structure.
Fig. 17. SEM image of bottom surface of body scale with small, irregularly arranged pores encircling the scale perimeter.
Fig. 18. SEM image of doubly serrated, twisted shaft base.
Fig. 19. SEM image of bottom surface of body scales.
Fig. 20. TEM image of body scale.
Fig. 21. TEM image of bristle.

submarginal ribs. The bristles covered the whole cell surface, were 6.3–12.1 μm long, and were slightly curved and twisted. The bristle shaft was ribbed with a row of doubly serrated teeth.

HOLOTYPE: Collection of specimens on SEM stub deposited at NNIBR, NNIBROR2.

STRAIN TYPE: Dongho031817J deposited at NNIBR, FBCC200021D.

TYPE LOCALITY: Dongho Beach, Dongho-ri, Haeri-myeon, Kochang-gun, Jellabukdo, Korea (35°31.00′N, 126°28.97′E), 18 March 2017.

ETYMOLOGY: The specific epithet '*marina*' refers to marine for their habitat.

Growth in various salinities

Cell counting and measurement of growth rates were performed in seven different salt concentrations (Figs 22–25). After transfer of both species to new media with different salinities, they grew well after 3 days (Figs 22, 24). At low salinities (0, 5 psu), they failed to grow throughout the experiment but were still alive. *M. cuspis* revealed the highest growth rate between salinities of 15 and 20 psu (μ = 0.69 day^{-1} and μ = 0.70 day^{-1}, respectively) and declined slightly at higher salinities (Figs 22, 23). The growth rate at 10 psu was lower than that at the other high-salinity cultures. *M. marina* showed a growth rate similar to that of *M. cuspis*. *M. marina* had a maximum growth rate at 20 psu (μ = 0.47 day^{-1}) and declined at higher salinities (Figs 24, 25). The growth rates at salinities of 10 and 15 psu were slightly lower than those in high-salinity cultures (Fig. 25). During the pre-adaption period, cell morphology was observed using light microscopy (LM; Figs 26–39). At low salinity (0, 5 psu), the cell shape of the two species was changed to spherical with an expanded chrysolaminarin vacuole. In addition, the plastid shape in both species became spherical and peripheral in each cell (Figs 26, 27, 33, 34). At other salt concentrations, the two species grew and had normal cell shapes (Figs 22–25, 28–32, 35–39).

DISCUSSION

The vast majority of *Mallomonas* species are distributed globally in freshwater ecosystems, but approximately 25 taxa of *Mallomonas* have been recorded from brackish water (> 5 psu) to almost full seawater (about 30 psu; Ikävalko 1994; Ikävalko & Thomsen 1996; Němcová *et al.* 2016). With the exception of *Mallomonas striata* Asmund, all species were found at a low salinity level of 5 psu (Ikävalko 1994). According to Ikävalko & Thomsen (1996), *M. striata* was found only at a high salinity of about 30 psu at Station 2, Bothnian Bay. *Mallomonas tolerans* was reported from many shallow, brackish pools in Alaska (Asmund & Hilliard 1965). The previously established strain *Mallomonas* sp. CCMP3275 (= *M. marina sp. nov.*) was isolated from Isonoura Beach, Wakayama, Japan, and *M. papillosa* CCMP476 was isolated from a salt marsh in England. Including *M. cuspis* and *M. marina* reported in this study, there are now 29 taxa known from brackish and coastal ecosystems. To our knowledge, only the three species *M. cuspis, M. marina* and *M. striata* live at salinities of 20–30 psu.

The scales of *M. cuspis* have a shallow, centrally positioned, V-shaped ridge on the broad shield, and irregularly spaced pores of various diameters across much of the scale except the anterior region. The scale does not have a dome, true V-rib, or other secondary structures. Based on scale morphology, *M. cuspis* is a member of the section *Planae*. Other members of the section *Planae* have different types of centrally positioned ridges. For example, *M. bangladeshica, M. ceylanica* and *M. peronoides* differ from *M. cuspis* by possessing much wider transverse ridges and papillae on the shield. In addition, phylogenetic analysis confirmed that *M. cuspis* is a member of the section *Planae*, with *M. heterospina* as a sister group.

Based on the phylogenetic analysis, *Mallomonas marina* grouped with members of the section *Striatae*, and characteristics of the scales confirmed this finding. Taxa in the section *Striatae* have similar characteristics, including hooded V-ribs, transverse ribs on the shield, dome with ribs or reticulations, and an anterior and posterior flange with struts. *M. marina* is similar in scale morphology to *M. cratis*. Both species have scales with U-shaped ribs on the dome, struts on the anterior and posterior flange, and well-formed hooded V-ribs. Interestingly, according to the original description of *M. cratis* (Harris & Bradley 1960), it was found in brackish pools behind sand or shingle near the sea. However, the diagnostic key characters of *M. marina* are large pores on the posterior flange and absence of teeth at the angle of the V-rib, more than 20 struts on the posterior flange, and curved or U-shaped ribs on dome. The phylogenetic analysis firmly supported that both isolated strains of *M. marina* are closely related to *M. cratis*. According to Němcová *et al.* (2016), the occurrence of six *Mallomonas* species, including *M. cratis*, correlates positively with low salinity (> 5 psu). Therefore, the ability of *M. marina* and *M. cratis* to grow in a salt environment may be a characteristic derived from their common ancestor, but *M. marina* seems to be better adapted to high salt concentrations than *M. cratis*.

Both new *Mallomonas* species grew at higher salinities than the 10 psu tested, showing a wide tolerance to salt levels. The two marine *Mallomonas* species showed the highest growth rate at 20 psu, and at low salinities (0, 5 psu) they failed to grow. LM images after the pre-adaption period showed abnormal cell morphologies at low salinities (0, 5 psu). We suggest that the expanded chrysolaminarin vacuole affacted plastid morphology and may affect other organelles as well. Our phylogenetic tree suggested that two *Mallomonas* species independently made a transition from freshwater to a brackish and/or marine environment. Because growth response of phytoplankton strains can differ between culture and field (Balzano *et al.* 2011; Lakeman *et al.* 2009), we do not know whether the two marine *Mallomonas* species also grow well in natural freshwater or brackish water environments. However, our data clearly revealed that both marine *Mallomonas* species lost the ability to adapt to freshwater or brackish water (> 5 psu); whereas, both species still had positive growth in higher salt environments (< 10 psu), indicating that they are marine species adapting to a range of high salinities.

In summary, the vast majority of *Mallomonas* species live in freshwater where they often form important components of phytoplankton communities. Here, we reported two

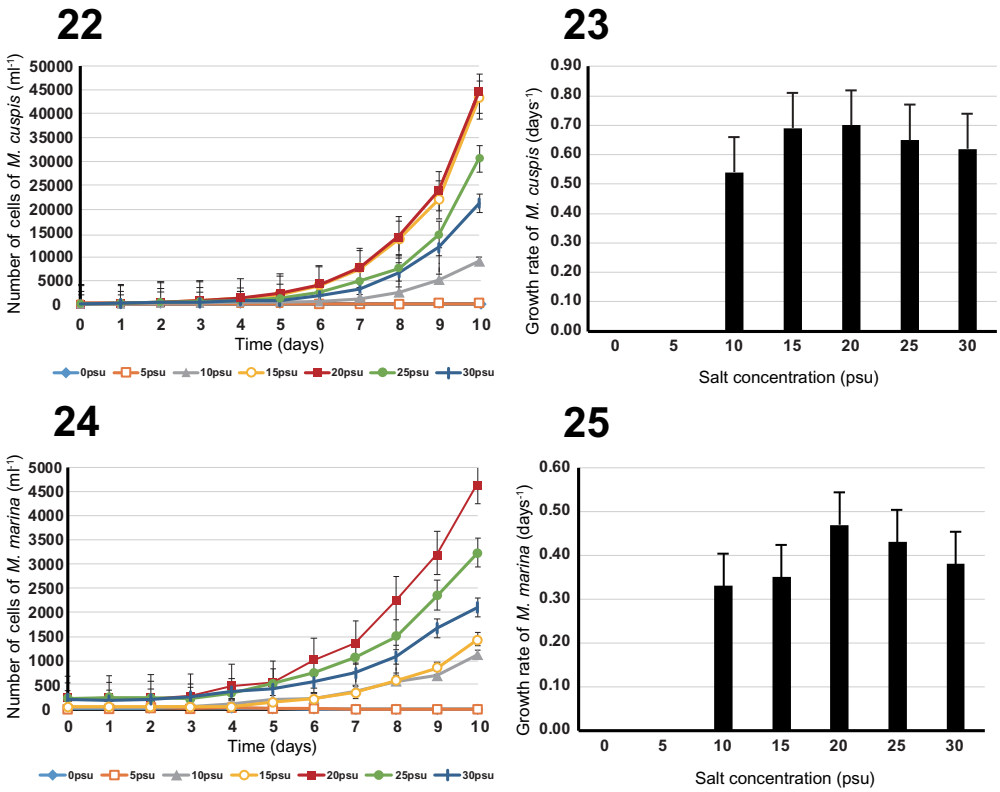

Figs 22–25. Effects of various salt concentrations on growth of two species of marine *Mallomonas*

Fig. 22. Daily cell counts of *M. cuspis* over a 10-day period indicating high cell numbers at 10, 15, 20, 25 psu, but no growth at 0 or 5 psu.

Fig. 23. Growth rate of *M. cuspis* versus salt concentration with high growth rates in cultures at 15 and 20 psu and then slightly declining at 25 and 30 psu.

Fig. 24. Daily cell counts of *M. marina* over a 10-day period. Cultures grown at 10, 20, 25, 30 psu have high cell numbers but those at 0 and 5 psu did not.

Fig. 25. Growth rates of *M. marina* in different salt concentrations with the highest growth rate at 20 psu and then declining at 25 and 30 psu.

.

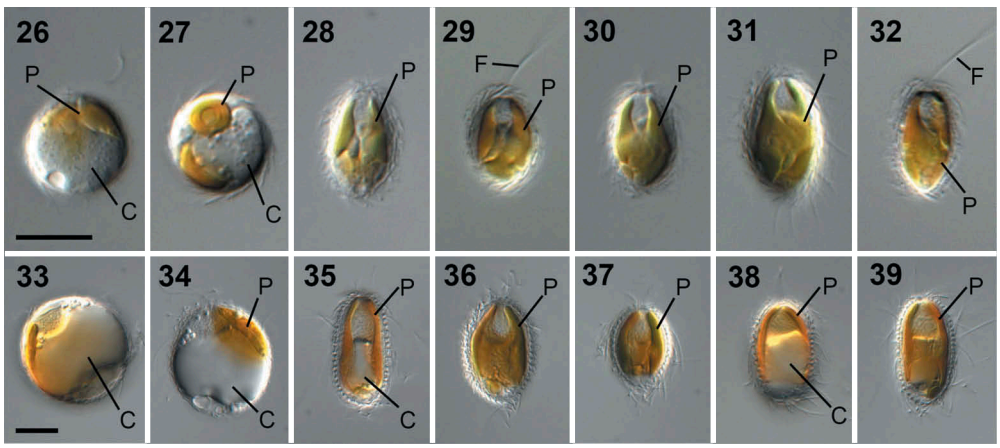

Figs 26–39. Light micrographs of *Mallomonas cuspis* Dongho022517B3 after 7 pre-adaption days in each salt concentration. C, chrysolaminrin vacuole; F, flagellum; P, plastid. Scale bar = 10 µm.

Fig. 26. Cell at 0 psu with spherical shape and expanded chrysolaminarin vacuole (C) and peripheral plastid (P).

Fig. 27. Cell grown at 5 psu showing spherical shape with expanded chrysolaminarin vacuole (C) and peripheral plastid (P).

Fig. 28. Cell grown at 10 psu salinity.

Fig. 29. Cell grown at 15 psu.

Fig. 30. Cell grown at 20 psu.

Fig. 31. Cell grown at 25 psu.

Fig. 32. Cell grown at 30 psu.

Figs 33–39. Light micrographs of *Mallomonas marina* Dongho031817J after 7 pre-adaption days in each salt concentration. C, chrysolaminrin vacuole; F, flagellum; P, plastid. Scale bar = 10 µm.

Fig. 33. Cell grown at 0 psu showing spherical shape with expanded chrysolaminarin vacuole (C) and peripheral plastid (P).

Fig. 34. Cell grown at 5 psu showing spherical shape with expanded chrysolaminarin vacuole (C) and peripheral plastid (P).

Fig. 35. Cell grown at 10 psu with typical cylindrical morphology; plastid (P) located on the edge of the cell and chrysolaminarin vacuole (C) in the cell posterior.

Fig. 36. Cell grown at 15 psu.

Fig. 37. Cell grown at 20 psu.

Fig. 38. Cell grown at 25 psu.

Fig. 39. Cell grown at 30 psu.

Mallomonas species, *M. cuspis* and *M. marina*, from a marine environment, doubling the number marine species. Based on growth rates, the two marine *Mallomonas* species can adapt to brackish environments but are best adapted to marine environments. Our phylogenetic analysis suggests that the two *Mallomonas* species moved independently from freshwater to a brackish or marine environment.

ACKNOWLEDGEMENTS

We thank two reviewers and Dr David Garbary for their significant contributions that substantially improved the article.

FUNDING

This research was supported by grants from the National Research Foundation (NRF) of Korea (NRF-2015R1A2A2A01003192 and NRF-2015-M1A5A1041808) and Nakdonggang National Institute of Biological Resources (NNIBR2018122) to W.S.

REFERENCES

Andersen R.A. 2007. Molecular systematics of the Chrysophyceae and Synurophyceae. In: *Unravelling the algae: the past, present, and future of algal systematics* (Ed. by J. Brodie & J. Lewis), pp. 285–313. CRC Press, Boca Raton, Florida, USA.

Andersen R.A., Berges J.A., Harrison P.J. & Watanabe M.M. 2005. Appendix A – recipes for freshwater and seawater media. In: *Algal culturing techniques* (Ed. by R.A. Andersen), pp. 457–458. Elsevier Academic Press, London, UK.

Asmund B. & Hilliard D.K. 1965. Studies on Chrysophyceae from some ponds and lakes in Alaska. IV. Occurrence of a *Mallomonopsis* species in brackish water. *Hydrobiologia* 26: 521–526. DOI: 10.1007/BF00045543.

Balzano S., Sarno D. & Kooistra W.H.C.F. 2011. Effects of salinity on the growth rate and morphology of ten *Skeletonema* strains. *Journal of Plankton Research* 33: 937–945. DOI: 10.1093/plankt/fbq150.

Dürrschmidt M. & Cronberg G. 1989. Contributions to the knowledge of tropical chrysophytes: Mallomonadaceae and Paraphysomonadaceae from Sri Lanka. *Archiv für Hydrobiologie Supplement 82 (1)/ Algological Studies* 54: 15–37.

Harris K. & Bradley D.E. 1960. A taxonomic study of *Mallomonas*. *Journal of General Microbiology* 22: 750–777. DOI: 10.1099/00221287-22-3-750.

Ikävalko J. 1994. Observation on silica-scaled flagellates (Chrysophyceae and Synurophyceae) in the brackish water of Pojo Bay, SW coast of Finland. *Annales Botanici Fenici* 31: 1–27.

Ikävalko J. & Thomsen H.A. 1996. Scale-covered and loricate flagellates (Chryosophyceae and Synurophyceae) from Baltic Sea ice. *Nova Hedwigia, Beiheft* 114: 147–160.

Jo B.Y., Shin W., Boo S.M., Kim H.S. & Siver P.A. 2011. Studies on ultrastructure and three-gene phylogeny of the genus *Mallomonas* (Synurophyceae). *Journal of Phycology* 47: 415–425. DOI: 10.1111/j.1529-8817.2010.00953.x.

Jo B.Y., Shin W., Kim H.S., Siver P.A. & Andersen R.A. 2013. Phylogeny of the genus *Mallomonas* (Synurophyceae) and descriptions of five new species on the basis of morphological evidence. *Phycologia* 52: 266–278. DOI: 10.2216/12-107.1.

Jo B.Y., Kim J.I., Škaloud P., Siver P.A. & Shin W. 2016. Multigene phylogeny of *Synura* (Synurophyceae) and descriptions of four new species based on morphological and DNA evidence. *European Journal of Phycology* 51: 413–430. DOI: 10.1080/09670262.2016.1201700.

Kristiansen J. 2002. The genus *Mallomonas* (Synurophyceae): a taxonomic survey based on the ultrastructure of silica scales and bristles. *Opera Botanica* 139: 1–218.

Kristiansen J. 2005. *Golden algae: a biology of chrysophytes*. A.R.G. Gantner Verlag, Ruggell, Lichtenstein. 163 pp.

Kristiansen J. & Preisig H.R. 2007. Chrysophyte and haptophyte algae. Part 2: Synurophyceae. In: *Süßwasserflora von Mitteleuropa freshwater flora of Central Europe* (Ed. by B. Büdel, G. Gärtner, L. Krienitz, H. R. Preisig & M. Schagerl), pp. 1–252. Springer-Verlag, Berlin.

Lakeman M.B., von Dassow P. & Cattolico R.A. 2009. The strain concept in phytoplankton ecology. *Harmful Algae* 8: 746–758. DOI: 10.1016/j.hal.2008.11.011.

Lavau S., Saunders G.W. & Wetherbee R. 1997. A phylogenetic analysis of the Synurophyceae using molecular data and scale case morphology. *Journal of Phycology* 33: 135–151. DOI: 10.1111/j.0022-3646.1997.00135.x.

Molecular evolution, phylogenetics and epidemiology. https://tree.bio.ed.ac.uk; searched on 20 July 2017.

National Center for Marine Algae and Microbiota at Bigelow Laboratory. https://ncma.bigelow.org; searched on 20 July 2017.

Němcová Y., Martin P., Škaloudová M. & Neustupa J. 2016. Silica-scaled chrysophytes (Stramenophile, Ochrophyta) along a salinity gradient: a case study from the Gulf of Bothnia western shore (northern Europe). *Hydrobiologia* 764: 187–197. DOI: 10.1007/s10750-015-2424-9.

Posada D. & Crandall K.A. 1998. MODELTEST: testing the model of DNA substitution. *Bioinformatics* 14: 817–818.

Ronquist F., Teslenko M., van der Mark P., Ayres D., Darling A., Höhna S., Larget B., Liu L., Suchard M.A. & Huelsenbeck J.P. 2012. MrBayes 3.2: efficient Bayesian phylogenetic inference and model choice across a large model space. *Systematic Biology* 61: 539–542. DOI: 10.1093/sysbio/sys029.

Siver P.A. 1991. *The biology of* Mallomonas*: morphology, taxonomy, and ecology*. Kluwer Academic Publishers, Dordrecht, Netherlands. 228 pp.

Siver P.A. 1993. Inferring the specific conductivity of lake water with scaled chrysophytes. *Limnology and Oceanography* 38: 1480–1492. DOI: 10.4319/lo.1993.38.7.1480.

Siver P.A. 2018. *Mallomonas aperturae sp. nov*. (Synurophyceae) reveals that the complex cell architecture observed on modern synurophytes was well established by the middle Eocene. *Phycologia* 57: 273–279. DOI: 10.2216/17-112.1.

Siver P.A. & Hamer J.S. 1989. Multivariate statistical analysis of the factors controlling the distribution of scaled chrysophytes. *Limnology and Oceanography* 34: 368–381. DOI: 10.4319/lo.1989.34.2.0368.

Siver P.A. & Glew J.R. 1990. The arrangement of scales and bristles on *Mallomonas*: a proposed mechanism for the formation of the cell covering. *Canadian Journal of Botany* 68: 374–380. DOI: 10.1139/b90-049.

Siver P.A., Wolfe A.P., Rohlf J., Shin W. & Jo B.Y. 2013. Combining geometric morphometrics, molecular phylogeny, and micropaleontology to assess evolutionary patterns in *Mallomonas* (Synurophyceae: Heterokontophyta). *Geobiology* 11: 127–138. DOI: 10.1111/gbi.12023.

Siver P.A., Jo B.Y., Kim J.I., Shin W., Lott A.M. & Wolfe A.P. 2015. Assessing the evolutionary history of the class Synurophyceae (Heterokonta) using molecular, morphometric and paleobiological approaches. *American Journal of Botany* 102: 921–941. DOI: 10.3732/ajb.1500004.

Smith S.W., Overbeek R., Woese C.R., Gilbert W. & Gillevet P.M. 1994. The Genetic Data Environment: an expandable GUI for multiple sequence analysis. *Computer Applications in the Biosciences* 10: 671–675.

Stamatakis A. 2014. RAxML version 8: a tool for phylogenetic analysis and post-analysis of large phylogenies. *Bioinformatics* 30: 1312–1313. DOI: 10.1093/bioinformatics/btu033.

Wuyts J., De Rijk P., Van de Peer Y., Winkelman T. & De Wachter R. 2001. The European large subunit ribosomal RNA database. *Nucleic Acids Research* 29: 175–177. DOI: 10.1093/nar/29.1.175.